The $SLAP_{TAG}$: A new molecular tag adapted for the development of a high-performance, low-cost, affinity chromatography system

Emanuel J. Muruaga[1,2], Paula J. Uriza[1,2], Gonzalo A. K. Eckert[1,2], María V. Pepe[1,2], Cecilia M. Duarte[1,2], Mara S. Roset[1,2] * and Gabriel Briones[1,2] *.

1. Instituto de Investigaciones Biotecnológicas, Universidad Nacional de San Martín (UNSAM)- Consejo Nacional de Investigaciones Científicas y Técnicas (CONICET). 2. Escuela de Bio y Nanotecnologías (EByN), Universidad Nacional de San Martín.

Running title: The $SLAP_{TAG}$ affinity chromatography (SAC)

Keywords: Affinity chromatography-$SLAP_{TAG}$.

*Corresponding author

Mailing address: Instituto de Investigaciones Biotecnológicas, Universidad Nacional de San Martín (IIB-UNSAM), Av. 25 de Mayo y Francia, Campus Migueletes, CP1650, San Martín, Buenos Aires, Argentina. Tel.: +54 11 4006-1500 (Int 2139); Fax: + 54 11 (5411) 4006-1559.

E-mail: gbriones@iib.unsam.edu.ar, mroset@iib.unsam.edu.ar

Abstract

The $SLAP_{TAG}$ is a novel molecular TAG derived from a protein domain present in the sequence of *Lactobacillus acidophilus* SlpA ($SlpA^{284-444}$). Proteins from different biological sources, with different molecular weights or biochemical functions, can be fused in frame to the $SLAP_{TAG}$ and efficiently purified by the specific binding to a bacterial-derived chromatographic matrix named here Bio-Matrix (BM). To set an optimized protocol for the $SLAP_{TAG}$-based affinity chromatography (SAC) different binding and elution conditions were evaluated. The binding equilibrium between $SLAP_{TAG}$ and BM was reached after a few minutes at 4°C, being the apparent dissociation constant (K_D) of 4.3 uM, a value similar to the one determined for other S-layer proteins and their respective bacterial cell-walls. A reporter protein was generated (H_6-GFP-$SLAP_{TAG}$) to compare the efficiency of SAC against a commercial system based on a Ni^{2+}-charged agarose matrix, observing no differences in the H_6-GFP-$SLAP_{TAG}$ purification performance. The stability and reusability of the BM were evaluated, and it was determined that the matrix was stable for more than a year, being possible to reuse it five times without a significant loss in the efficiency for protein purification. Alternatively, we explored the recovery of bound SLAP-tagged proteins by proteolysis using the $SLAP_{ASE}$ (a SLAP-tagged version of the HRV-3c protease) that released a tag-less GFP ($SLAP_{TAG}$-less). Additionally, iron nanoparticles were linked to the BM and the resulting BM_{mag} was successfully adapted for a magnetic SAC, a technique that can be potentially applied for high-throughput-out protein production and purification.

38 **Main**

39 The amalgamation of genomics, transcriptomics, proteomics, metabolomics, synthetic biology, and artificial
40 intelligence has become a powerful approach to understand the complexity of any biological process,
41 uncovering uncharacterized molecular mechanisms [1 2 3].

42 In addition to being central for scientific research, OMICs also have become the core of the
43 biomanufacturing platform oriented to the generation of bioproducts of commercial value (either new
44 products or biosimilars) [4]. Amidst the universe of bioproducts, therapeutic proteins are a growing class of
45 biopharmaceutics that are being used for cancer, autoimmunity, and inflammatory diseases [5].

46 Because of their clinical efficiency and low toxicity, therapeutic proteins (monoclonal antibodies, cytokines,
47 antigens, hormones, vaccines, etc.) have become an excellent option for different ailment treatments [6 7].
48 However, one of the limitations these treatment face is the high cost of manufacturing, which has
49 bottlenecked therapeutic protein production and promoted the development of several strategies to
50 improve the upstream and downstream processes [7].

51 The downstream process includes all the purification steps oriented to capture and eliminate protein
52 aggregates and any remanent impurities derived from the host cell (e.g., DNA), preserving the biological
53 activity of the purified bioproduct. At the core of the downstream process, chromatography is the critical
54 step but also the most expensive one [8 9]. To reduce critical costs associated with this step different
55 approaches have been evaluated including the adoption of single-use technologies [10].

56 Affinity chromatography is a special type of liquid chromatography that exploits the existence of natural [11]
57 or artificial [12] affinities between two moieties: the molecular target (or tag) and its ligand (the affinity ligand)
58 which is usually immobilized onto a chromatographic stationary phase to generate a chromatography
59 matrix. Thus, proteins of interest can be fused in frame to different molecular tags (such as His-6X, GST,
60 MBP, etc.) expressed and purified ideally in a single step from a complex mixture of proteins.

61 Since it was developed by Starkestein in 1910 [13], affinity chromatography was gaining popularity and
62 centrality for many industrial processes such as the purification of proteins for diagnosis, research, and
63 therapeutic purposes [14]. Regulatory requirements for the purity and quality of the proteins varies greatly
64 depending on the area of application. For instance, for industrial use, bio-products can be used with little
65 purification. Also, recombinant protein produced for research, diagnosis, or non-clinical purposes have a
66 less stringent regulatory approval process than proteins designed as biopharmaceuticals.

67 Here, we explored the adaptation of a protein domain present in the carboxy terminus of the *Lactobacillus*
68 *acidophilus* protein SlpA as a molecular tag. *In silico* analysis of this region ($SlpA^{284-444}$) allowed us to identify
69 a tandem of two copies of a 60-aminoacid protein domain named SLP-A (pfam03217) which is necessary
70 for the association. Here, this dual SLP-A domain was named $SLAP_{TAG,}$ and the adaptation as a molecular tag
71 was evaluated. Recently, we have characterized the binding properties of the $SLAP_{TAG}$ and characterized
72 its association to live *Lactobacillus* wall for vaccine purposes [15]. Thus, the $SLAP_{TAG}$ was fused in frame to a
73 chimeric antigen derived from the Shiga toxin-producing *Escherichia coli* (STEC) formed by the peptides
74 $EspA^{36–192}$, $Intimin^{653–953}$ and $Tir^{240–378}$ (or EIT). The resulting chimeric antigen (EIT-$SLAP_{TAG}$) recombinantly
75 expressed and purified was able to associate to the bacterial cell-wall of *L. acidophilus*, a process that we
76 named decoration. Thus, EIT-decorated *L. acidophilus* after oral administration was able to deliver the EIT
77 antigen to the intestinal mucosa eliciting a protective immune response that controls an experimental STEC
78 infection in mice [15]. Remarkably, the decoration process does not modify genetically the *Lactobacillus*
79 genome preserving its GRAS (Generally Recognized as Safe) status, a trait that is important for vaccine
80 purposes.

81 Here, we explore the adaptation of the $SLAP_{TAG}$ for the development of a novel affinity chromatography,
82 the SLAP affinity chromatography (SAC), and a comprehensive protocol is presented.

83 **Results**

84 **$SLAP_{TAG}$ binds rapidly and efficiently to the Bio-matrix (BM)**

85 As described in Materials and Methods the $SLAP_{TAG}$ was fused in-frame to the carboxy-terminus of the green
86 fluorescent protein (GFP) to generate the chimeric protein (H_6)-GFP-$SLAP_{TAG}$ adapted here as a $SLAP_{TAG}$
87 reporter protein. As shown in Fig. 1A the structure of the chimeric protein (H_6)-GFP-$SLAP_{TAG}$ was predicted
88 based on alphaFold-2 method [16]. The beta-barrel corresponding to GFP and the two globular domains
89 corresponding to $SLAP_{TAG}$ were predicted with high performance and as expected, linkers and 6xHis-tag,
90 which are flexible regions, showed low prediction values.

91 As a working chromatographic matrix, a culture of *Bacillus subtilis* natto was processed as described in
92 Materials and Methods to generate a bacterial-derived affinity chromatography matrix, named here Bio-
93 Matrix (BM). Interestingly, although *B. subtilis* has no S-layer, we have demonstrated previously that this
94 bacterium can be externally covered with SLAP-tagged proteins to generate a recombinant S-layer on its
95 bacterial cell wall, a process that we called decoration [15]. Decoration of *B. subtilis* with SLAP-tagged proteins
96 is possible because teichoic acid and lipoteichoic acid (which are the molecules responsible for $SLAP_{TAG}$
97 association) have the same chemical composition than *Lactobacillus acidophilus*. Interestingly, in *B. subtilis*
98 and *L. acidophilus* teichoic acid and lipoteichoic acid are distributed homogeneously on their cell wall.

99 To characterize the binding properties of the $SLAP_{TAG}$, the reporter protein (H_6)-GFP-$SLAP_{TAG}$, was
100 recombinantly expressed in *Escherichia coli*, purified by affinity chromatography mediated by its Hisx6 tag
101 (H_6), and further incubated with BM under a variety of conditions. Initially, as shown in Fig. 1B, the optimal
102 binding temperature of (H_6)-GFP-$SLAP_{TAG}$ to the BM was evaluated, finding that the best binding efficiency
103 was reached when the incubation was performed at 4°C. To get insights into the $SLAP_{TAG}$ association
104 dynamics, (H_6)-GFP-$SLAP_{TAG}$ was incubated for 5, 30 and 60 minutes with BM and as shown in the Fig. 1C,
105 the maximal binding of (H_6)-GFP-$SLAP_{TAG}$ to BM was reached very rapidly (already at 5 minutes), showing
106 no significant increments in its association at longer time points. These results indicated that the $SLAP_{TAG}$
107 binds very rapidly and with an apparent high affinity to the BM. To quantify the affinity of the interaction

108 between the $SLAP_{TAG}$ with the BM, an adsorption isotherm was performed to determine the equilibrium
109 apparent dissociation constant as described in Materials and Methods. As shown in Fig. 1D the apparent K_D
110 was estimated as 4.7 uM. Interestingly, this dissociation constant value was in the same order than other
111 K_D described for different microbial S-layer proteins with their respective bacterial walls [17–19]. In addition,
112 the maximum adsorption capacity (Bmax) of BM was estimated as 1.152 mmols of (H_6)-GFP-$SLAP_{TAG}$ or 53.9
113 mg of protein per milliliter of BM or 1.03 g of $SLAP_{TAG}$ protein/g of dry BM.

114 **Elution of (H_6)-GFP-$SLAP_{TAG}$ protein can be performed with different buffers**

115 As it was mentioned, the $SLAP_{TAG}$ contains the protein region responsible for the association of the protein
116 SlpA to the *L. acidophilus* cell wall. As reported, *L. acidophilus* SlpA has the natural ability to self-assemble
117 on the bacterial surface to generate a proteinaceous layer named S-layer [20], a highly ordered wall structure
118 that functions as a protective barrier against bacteriophages, resistance to low pH and proteases, and
119 bacterial adhesion. It is well characterized that remotion of the S-layer can be performed efficiently by the
120 addition of chaotropic agents like LiCl, a compound that disrupts hydrogen bonds leading to a partial
121 denaturation of proteins and the consequent detachment of the S-layer [20]. Thus, initially, to study elution
122 conditions for (H_6)-GFP-$SLAP_{TAG}$, LiCl solution was selected as the positive control for elution and as shown
123 in Fig. 2A detachment of BM-associated (H_6)-GFP-$SLAP_{TAG}$ was achieved with high efficiency with a 2M LiCl
124 solution at room temperature, in a short lapse of five minutes (Fig. 2B). As it was mentioned above, lithium
125 solutions have deleterious effects on proteins, which is an undesired effect for protein purification,
126 especially for enzyme purification. Therefore, different milder alternatives of buffers were explored to elute
127 $SLAP_{TAG}$-tagged proteins, conditions that can preserve the protein structure and therefore their function.
128 As shown in Fig. 2C, a series of sugars (monosaccharide and disaccharides) described previously [21] were
129 tested for the elution of the reporter SLAP observing a partial elution efficiency when compared with the
130 LiCl elution control (Fig. 2C). Next, the cationic nature of the $SLAP_{TAG}$ at neutral pH was considered. Taking
131 in consideration the importance of this positive charge in the interaction of $SLAP_{TAG}$ with the membrane-
132 bound compound teichoic acid, a set of cationic compounds was evaluated for the elution. As shown in Fig.

133 2C, 0.3M of CTAB was able to elute (H_6)-GFP-SLAP$_{TAG}$ with a similar efficiency as the LiCl solutions. Although
134 CTAB was very efficient in this step, we found that this compound was difficult to remove downstream from
135 the elution fraction. Then, considering that SLAP$_{TAG}$ has a theoretical isoelectric point (pI) value of 9.92, we
136 explored if the modification of pH can be adapted as an elution method. As shown in Fig. 2C, when the pH
137 of the bicarbonate buffer was close to the theoretical SLAP$_{TAG}$ isoelectric point (pI), (H_6)-GFP-SLAP$_{TAG}$ was
138 efficiently eluted from BM. In addition, after establishing the bicarbonate buffer at pH 10 as an elution
139 buffer, we explore if the addition of NaCl can improve the elution process. As shown in Fig. 2C, the addition
140 of 200 mM of NaCl was able to maximize the yield of recovery of (H_6)-GFP-SLAP$_{TAG}$ in the eluate.

141 **Optimized SAC protocol allowed the efficient purification of proteins with similar efficiency to the high-**
142 **performance Ni^{2+}-charged agarose matrix (IMAC).**

143 With all the experimental information obtained, an optimized SAC protocol for the purification of SLAP-
144 tagged proteins was established as shown in Fig. 3A. Remarkably, the entire process of protein purification
145 can be performed in 15 minutes. To have a direct observation of the purification process of (H_6)-GFP-
146 SLAP$_{TAG}$, the BM was fixed and immobilized on coverslips at different steps of the process to be observed
147 by confocal microscopy. As shown in Fig. 3B, before the incubation of BM with (H_6)-GFP-SLAP$_{TAG}$, only a red
148 native autofluorescence can be observed from fixed *Bacillus subtilis* natto cells present in BM. Remarkably,
149 after the incubation of BM with (H_6)-GFP-SLAP$_{TAG,}$ it was possible to detect the adhesion of the reporter
150 protein to the BM forming a recombinant fluorescent S-layer that covers completely the bacterial surface
151 (Fig. 3C). As expected, after the addition of the elution buffer the (H_6)-GFP-SLAP$_{TAG}$ was completely removed
152 from the bacterial surface (Fig. 3D). In addition, the whole process of purification can also be monitored by
153 direct observation under UV light (Fig. 3E)

154 Since SAC was efficient in protein purification, we compared this new technique against an established
155 affinity purification protocol. For this, we took advantage that (H_6)-GFP-SLAP$_{TAG}$ also has an His-tag that can
156 be purified by a Metal-Affinity-Chromatography or IMAC. As described in Materials and Methods, a
157 bacterial lysate (H_6)-GFP-SLAP$_{TAG}$ was divided into two fractions and both protocols were performed

158 accordingly, confirming that SAC optimized protocol was able to purify (H_6)-GFP-SLAP$_{TAG}$ with high efficiency
159 (Table Suppl. 1 and Fig. 3F) and with a similar yield to the one obtained with the commercial IMAC (Fig. 3G).

160

161 **Proteins of different biological sources, molecular weights, biochemical functions, or expressed by**
162 **procaryotic or eukaryotic expression systems can be efficiently purified by the SAC.**

163 To evaluate if SLAP$_{TAG}$ and SAC can be adapted as a universal protein purification system, a set of the
164 selected proteins were fused to the SLAP$_{TAG}$ (Fig. 4). Thus, bacterial proteins like *Salmonella* flagellin
165 (Fig.5A), the STEC proteins, EspA (Fig. 5B), the chimeric EIT (Fig. 5C) , the *B. abortus* Omp19 (Fig. 5D), the
166 bacteriophage protein T7-lysozyme (Fig. 5E), the human viral proteins Rhinovirus 3C Protease (Fig. 5E), the
167 mouse Galectin-8 (Fig. 5G) and the commercial molecular tag GST (Fig. 5H), were fused in frame with the
168 SLAP$_{TAG}$. As shown in Fig. 5, all the selected proteins were purified efficiently with SAC. In addition to the
169 bacterial expression system, different protein expressions systems (yeast and mammalian cells) were also
170 evaluated (Fig. 6). As shown in Fig. 6A the viral HRV 3C protease fused to the SLAP$_{TAG}$ was expressed and
171 purified from *Pichia pastoris* supernatant. Also, the SARS-CoV2 SPIKE fused to the SLAP$_{TAG}$ was purified
172 from the supernatant of transfected HEK293 (Fig. 6B). These results confirmed that the SLAP$_{TAG}$ can be
173 widely adopted for affinity chromatography purification.

174

175 **BM is a reusable chromatography matrix with long-term stability.**

176 As described in Materials and Methods a batch of BM was produced, and several aliquots were frozen at -
177 20°C to study time stability. As shown in Fig. 7A, at different times, a few aliquots were unfrozen and tested
178 for protein purification of the reporter protein (H_6)-GFP-SLAP$_{TAG}$ being the BM stable for more than a year
179 (14 months). In addition, BM reusability capacity was evaluated determining that the matrix can be reused
180 five times with no modification of the protein purification yield (Fig. 7B).

181

182 **Use of the Human Rhinovirus 3C protease fused to the $SLAP_{TAG}$ ($SLAP_{ASE}$) to release the SLAP-tagged**
183 **proteins from BM.**

184 As shown in Fig. 4 and 5 sequence of the viral protease HRV-3C was fused to the $SLAP_{TAG}$ (named $SLAP_{ASE}$),
185 recombinantly expressed, and purified (Fig. 8B and 8D, lane SLAPase) to evaluate its activity. A reporter
186 protein for $SLAP_{ASE}$ activity was generated (GFP-LEVLFQGP-$SLAP_{TAG}$) (Table 1) and a protocol for tag-remotion
187 by SLAPase was set as described in Materials and methods. As shown in Fig. 8A the GFP-LEVLFQGP-$SLAP_{TAG}$
188 was expressed (Fig 8B and Fig. 8C , lane Input or IN) and mixed with the BM for 5 minutes allowing the
189 binding process. After binding, a purified $SLAP_{ASE}$ was added to the mix and incubated for 60 minutes
190 releasing a tag-less GFP (Fig. 8B and Fig 8C, Fig 8E, lanes flow-through or FT) by proteolysis. Cut $SLAP_{TAG}$ is
191 not observed in the flow-through indicating that was retained by the BM along with the SLAPase. To confirm
192 these steps, post-proteolysis BM was incubated with LiCl solution to remove any residual bound SLAP-
193 tagged protein. As shown in Fig. 8B and 8D (lane Elution or E), the LiCl solution released the SLAPase and
194 the cut $SLAP_{TAG}$.

195

196 **Adaptation of SAC to a magnetic affinity chromatography.**

197 Since we confirmed the efficiency and universality of SAC for the purification of recombinant proteins, we
198 explored a magnetic affinity chromatography SAC alternative (Fig. 9A). As shown in Fig. 9B, 9C and
199 Supplementary Video-1 the (H_6)-GFP-$SLAP_{TAG}$ was purified in a few and easy steps. As shown in the SDS-
200 PAGE (Fig. 9B) the adapted SAC protocol for magnetic chromatography (BM_{mag}) was able to purify the
201 reporter protein (H_6)-GFP-$SLAP_{TAG}$ very efficiently (Fig. 9B , lane Elution or E). Interestingly, this protocol can
202 be adapted to commercial devices that use magnetic force for protein or DNA purification (like King Fisher
203 Flex from ThermoFisher). In Fig. 9C the entire process of purification was monitored by direct observation
204 under UV light (Supp. video 1). Noteworthy, the binding of the BM_{mag} to GFP quenched the fluorescence of
205 this protein, an effect that was described for transition metal binding to GFP or binding of iron cations to
206 fluorescent proteins (Fig. 9C, tube IN+BM_{mag}) [22,23].

207 **DISCUSSION**

208 Proteins are macromolecules formed by a particular amino acid sequence that determines a given atomic
209 spatial distribution, also known as protein conformation. Far from being a rigid structure, proteins behave
210 as nano-machines performing precise molecular activities because of the internal movements of protein
211 parts or protein domains. Proteins can interact intramolecularly or intermolecularly with different
212 macromolecules such as proteins, DNA, RNA, polysaccharides, or with small compounds [24]. Some proteins
213 degrade aliments to produce essential nutrients (like the digestive enzymes), proteins that transport critical
214 compounds for supporting life (like hemoglobin that transports oxygen to the cells), proteins that shape
215 the cellular structure (like actin, tubulin or keratin), proteins that function as hormones (like insulin),
216 proteins that defense the organisms against pathogens (like the antibodies) [24]. In addition to the multiplicity
217 of existent polypeptides in nature, molecular biology and biotechnology have generated a myriad of
218 chimeric proteins by combining different protein domains [25]. These artificial proteins can be used as
219 therapeutic tools to treat cancer, autoimmunity, or different medical conditions [26].

220 The SARS-CoV-2 pandemic has generated a multidimensional global crisis with devastating effects on
221 human health, also having a massive impact on the economics everywhere. As a direct consequence of this
222 global disaster, national governments were thrown into a global raging competition to acquire all the
223 required medical supplies. In addition to the shortage of masks or ventilators, the huge demand for
224 diagnostic reagents (such as recombinant proteins) has bottlenecked the development of new viral
225 diagnosis kits based on ELISA or Real-time PCR tests.

226 Among all other things, the pandemic crisis had taught us that the availability of low-cost affinity
227 chromatography might be a helpful tool for producing pure recombinant proteins to develop low-cost
228 diagnostics tests.

229 Here we propose the adaptation of the binding domain of the *Lactobacillus acidophilus* SlpA as a molecular
230 tag. As it was shown here, SAC is a useful tool for protein purification because i) SAC protocol uses only
231 simple and low-cost reagents, ii) the chromatography matrix is ¨grown¨ instead of being chemically

232 synthetized, iii) ligands (LTA and teichoic acid) are naturally integrated to surface of the BM with no need
233 of chemical reactions to crosslink them to the matrix.

234 In summary, we propose that SLAP affinity chromatography can be adapted as an in-house protein
235 purification system, available for any Laboratory around the globe, to produce pure recombinant proteins
236 for research, diagnosis, and for the food industry. Although so far regulatory issues might preclude the use
237 of the SAC for proteins used as biotherapeutics, new efforts have been performed to develop a new version
238 of the matrix chromatography suitable for more stringent industrial or clinical purposes.

239

240 **METHODS**

241 *Strains, plasmids, and transformation*

242 Bacterial strains and plasmids used here are summarized in Table 1. *Escherichia coli* and *Bacillus subtilis*
243 strains were grown in Luria Bertani (LB) medium (Sigma, St. Louis, MO, United States) at 37ºC 180 rpm.
244 Bacterial plasmid vectors were transformed in *E. coli* DH5α or in *E. coli* BL21 (DE3) for protein expression.
245 *Pichia pastoris* was grown in Yeast Extract–Peptone–Dextrose (YPD) medium at 28ºC 180 rpm. HEK293F cells
246 were grown and maintained at 0.5–3.0 × 10^6 cells/mL in a humidified CO_2 platform shaker incubator at 37 ºC
247 in Dulbecco's Modified Eagle's Medium (DMEM - ThermoFisher). SARS-CoV-2 was a gift from Jason McLellan
248 (Addgene # 154754; http://n2t.net/addgene:154754;RRID: addgene_154754) [27].

249 *Cloning*

250 Lysozyme gene was amplified from pLysS plasmid (Millipore Sigma-Novagen) with oligonucleotide primers
251 Fw-lys-*Nde*I (CCCATATGGCTCGTGTACAGTTTAAACAACGTG) and Rv-lys-SalI
252 (CGGTCGACTCCACGGTCAGAAGTGACCAGTTCG). The PCR product was digested with *Nde*I and *Sal*I and then
253 cloned into the pLC3-EITH7-SlpA vector at the *Nde*I and *Sal*I restriction sites. The recombinant plasmid was

254 amplified through transformation into *E. coli* DH5α. Finally, the lysozyme gene was subcloned into pET28-e
255 GFP-SlpA at the *Nde*I and *Not*I restriction sites and transformed into *E. coli* BL21 by electroporation.

256 *EspA* gene was amplified with the following primers: *pRvEspAXbaI* (GCTCTAGATTTACCAAGGGATATTGCTG)
257 *and pFwEITSalI* (ACGCGTCGACGATATGAATGAGGCATCTAAA). After restriction with *Xba*I and *Sal*I, the gene
258 was cloned into *pGEX-SlpA,* which was previously digested with the same enzymes. The plasmid was
259 introduced by electroporation into *E. coli* BL21.

260 The *hrv-3c-slap*$_{tag}$ gene was synthesized and cloned in pMAL-c5X and pPICZalfa B for protein expression in *E.*
261 *coli* and *P. pastoris* respectively (Gene Universal, Delaware-USA).

262 For *P. pastoris* GS115 transformation, 5 ug of pPICZalfa B – *hrv-3c* plasmid was linearized with *Sac*I restriction
263 enzyme and transformed into cells through electroporation using 2 mm gap cuvettes (1500 V, 125 X, 50 lF).
264 The transformed cells were selected by seeded on a YPD medium containing Zeocin 100ug/ml for resistance
265 selection. Colonies were further grown in test tubes containing YPD broth and after 24 h, cultures were
266 induced by adding 1% (v/v) pure methanol every 24 h (1). Supernatants were sampled after 72 h of induction
267 and the best producers were chosen for further experiments.

268 pET28-eGFP-SLAP was amplified and the SLAP$_{TAG}$ sequence subcloned into SARS-CoV-2 S HexaPro plasmid
269 (Addgene#154754) between *BamH*I and *Xho*I restriction sites.

270 *Protein expression*

271 *E. coli* BL21 were grown at 37ºC 180 rpm in liquid LB supplemented with antibiotics until they reached OD_{600}
272 = 0.6. Then, 0.1 mM IPTG was added, and bacteria were grown for another 20 hours at 18ºC 180 rpm. Finally,
273 bacteria were harvested and lyzed by sonication. The bacterial lysates were centrifuged for clarification.

274 *Pichia pastoris* protein expression was induced with methanol. Briefly, *P. pastoris* cultures were grown in 50
275 ml of YPD for 48 h. until dextrose was consumed. Then, 200 ul methanol pulses were supplied every 24 h for
276 5 days. Finally, *P. pastoris* were harvested, and supernatants were collected.

277 HEK cells were transfected using polyethyleneimine (PEI) for protein expression. Briefly, 30000 cells per well
278 were seeded in 24 well plates and incubated at 37 ℃, 5% CO_2 for 24 h. For transfection, 4 ul of PEI were
279 diluted in 40 ul of DMEM. 500 ng of DNA was added, and the transfection mix was incubated for 20 min at
280 room temperature. Then, the transfection mix was transferred to the cells and incubated for 48 h. Finally,
281 the supernatant was collected to check protein expression.

282 *6xHis-Tag purification method*

283 Purification of 6xHis-tagged proteins was carried out according to the manufacturer's protocol. Briefly,
284 benchtop columns were equilibrated with buffer (200 mM NaCl, 50 mM Tris-HCl pH 7.5). Columns were
285 loaded with clarifies of bacterial extracts. After being washed, columns were eluted in steps with 10, 50, 100,
286 300, and 500 mM imidazole in the equilibration buffer.

287 To be compared with Bio-Matrix system, the IMAC batch protocol was performed. Ni-NTA superflow resin
288 (Qiagen) was equilibrated with buffer (200 mM NaCl, 50 mM Tris-HCl pH 7.5) in 1,5 ml tubes. Clarifies of
289 bacterial lysate were loaded and mixed in an orbital shaker for 1 hour at 4ºC. Samples were centrifugated
290 and, after being washed, the resin was eluted with 500-mM imidazole in equilibration buffer.

291 *Bio-Matrix preparation*

292 *B. subtilis* were grown in 200 mL of Luria-Bertani broth at 37ºC 180 rpm for 48 hrs. Then, the culture was
293 centrifugated and the bacteria were washed twice with PBS. The culture was resuspended in PBS with 2%
294 glutaraldehyde and incubated overnight with soft agitation. Next, fixed bacteria were washed twice with PBS
295 and stored in 20 % ethanol.

296 BM was weighted in a drying scale (KERN MLS-D) and a calibration curve for dry weight vs optical density was
297 performed.

298 *$SLAP_{TAG}$ purification method*

299 To purify the SLAP-tagged proteins, Bio-Matrix was equilibrated in binding buffer (200 mM NaCl, 50 mM Tris-
300 HCl pH 7.5). Then, samples were incubated with the Bio-Matrix at different times and temperatures. Samples
301 were centrifuged (8000 rpm) and the Bio-Matrix was washed 3 times with binding buffer. Finally, samples
302 were incubated at different times and temperatures with the corresponding solution for elution. Proteins
303 expressed in HEK293 and *P. pastoris* were purified from the supernatant with the final protocol described in
304 this paper.

305 *Protein analysis*

306 Protein samples were dissolved in a cracking buffer and incubated for 5 min at 100ºC. Protein electrophoresis
307 was performed at 120V on 12% SDS-PAGE gel. Gels were stained in a Coomassie-Blue solution (20%
308 methanol, 10% acetic acid).

309 For Western Blot analysis, proteins were transferred to a nitrocellulose membrane for 55 min at 15V using a
310 semi-dry electroblotting transfer unit (Bio-Rad, Hercules, CA, United States). Membranes were incubated for
311 1 hour with blocking buffer (1% dry skim milk, 0,1% Tween in PBS). Then, membranes were incubated for 1
312 hour with primary antibody diluted in blocking buffer (1/500). After washing with PBS-0,1% Tween,
313 membranes were incubated for 1 hour with IRDye fluorophore-labeled secondary antibodies (LI-COR, Lincoln,
314 NE, United States) diluted in a blocking buffer (1/20000). Finally, membranes were scanned using the Odyssey
315 Imaging System (LI-COR).

316 *Fluorescence measurements*

317 GFP fluorescence measurements were performed at 485/535nm excitation-emission wavelength
318 respectively using FilterMax F5 Microplate Reader in Black 96 Well Plates (Thermo).

319 *Protein modeling*

320 (H_6)-GFP-SLAP$_{TAG}$ structure was predicted by AlphaFold[28]. ColabFold web interface was employed using
321 standard settings (five models and no templates).

322 *Adsorption isotherm*

323 Adsorption isotherms for (H_6)-GFP-SLAP$_{TAG}$ on Bio-Matrix were performed using batch experiments. BM was
324 equilibrated with binding buffer (50 mM Tris-HCl, 200 mM NaCl, and pH 7.6). Purified (H_6)-GFP-SLAP$_{TAG}$
325 protein at 3 mg/ml in binding buffer was used as a stock solution. Different concentrations of protein were
326 incubated with 10 ul of BM. After reaching equilibrium, samples were centrifugated and GFP fluorescence
327 from the supernatant was measured. Unbound protein in equilibrium with the BM was calculated using GFP
328 fluorescence. Bound protein was estimated by the difference between input and unbound protein. The
329 adsorption isotherm data were then fitted to the Langmuir isotherm equation to calculate the parameters
330 Qmax and K_D.

331 *Confocal Fluorescence Microscopy*

332 Samples were incubated for 30 min in plates treated with poly-L-Lysine (Sigma, St. Louis, MO, United State).
333 After treatment with PFA (4% in PBS), samples were washed twice with PBS. Finally, samples were observed
334 with a confocal laser-scanning microscope Olympus FV1000 using a PlanApo N (60 × 1.42 NA) oil objective.

335 *Cleavage of SLAP$_{TAG}$ with SLAP$_{ASE}$ protease*

336 Cleavage buffer recommended for commercial HRV3c protease was prepared: 50 mM Tris-HCl, pH 7.0, 150
337 mM NaCl, 1 mM EDTA, and 1 mM dithiothreitol. GFP-LEVLFQGP-SLAP$_{TAG}$ protein was bound to the Bio-Matrix.
338 The sample was washed with cleavage buffer at 4ºC. The protease SLAP$_{ASE}$ was added and incubated at 4ºC.

339 Percolate containing GFP protein without $SLAP_{TAG}$ was recovered. As a control, the protease and $SLAP_{TAG}$ were
340 eluted with Bio-Matrix elution buffer after cleavage.

341 *Synthesis of iron nanoparticles*

342 Iron nanoparticles were synthesized by reverse co-precipitation as described by Nadi et al [29] . In summary,
343 the precursor was prepared by dissolving 0.89 g of FeCl2.4H2O in 90 mL of water. The sample was incubated
344 in stirring for 15 min and sonicated for 10 min to ensure complete dissolution of the salt. The solution was
345 then poured over a solution of ammonium hydroxide diluted 1:2 with water and stirred for an hour. Finally,
346 the sample was washed repeatedly with deionized water.

347 *Magnetic Bio-Matrix generation*

348 Briefly, 5 ml of Bio-Matrix were resuspended in PBS and iron nanoparticles were added at a final
349 concentration of 40 g/L. The sample was mixed with gentle stirring for 30 minutes. Then, it was washed
350 repeatedly with PBS 1X and preserved in 20% ethanol.

351 *Antibody generation*

352 Mice were intraperitoneally injected with 10 ug of purified GST-$SLAP_{TAG}$ or GFP in aluminum hydroxide (Imject
353 Alum ThermoFisher). Two and four weeks later, booster doses of 5 ug of protein were administrated.

354 *Statistical analysis*

355 Statistical analyses were performed using GraphPad Prism 9 software. Statistical significance was analyzed
356 by one-way ANOVA with Bonferroni.

357

358 **References**

359 1. Cai, Z., Poulos, R. C., Liu, J. & Zhong, Q. Machine learning for multi-omics data integration in cancer.
360 *iScience* **25**, 103798 (2022).

361 2. Hassan, M. *et al.* Innovations in Genomics and Big Data Analytics for Personalized Medicine and
362 Health Care: A Review. *Int. J. Mol. Sci.* **23**, (2022).

363 3. Cong, Y. & Endo, T. Multi-Omics and Artificial Intelligence-Guided Drug Repositioning: Prospects,
364 Challenges, and Lessons Learned from COVID-19. *Omi. A J. Integr. Biol.* **26**, 361–371 (2022).

365 4. Amer, B. & Baidoo, E. E. K. Omics-Driven Biotechnology for Industrial Applications. *Frontiers in*
366 *Bioengineering and Biotechnology* vol. 9 at https://doi.org/10.3389/fbioe.2021.613307 (2021).

367 5. Zhu, M. M., Mollet, M., Hubert, R. S., Kyung, Y. S. & Zhang, G. G. Industrial Production of Therapeutic
368 Proteins: Cell Lines, Cell Culture, and Purification. in *Handbook of Industrial Chemistry and*
369 *Biotechnology* 1639–1669 (Springer International Publishing, 2017). doi:10.1007/978-3-319-52287-
370 6_29.

371 6. Lu, R. M. *et al.* Development of therapeutic antibodies for the treatment of diseases. *Journal of*
372 *Biomedical Science* vol. 27 at https://doi.org/10.1186/s12929-019-0592-z (2020).

373 7. Narayanan, H., Sponchioni, M. & Morbidelli, M. Integration and digitalization in the manufacturing
374 of therapeutic proteins. *Chem. Eng. Sci.* **248**, 117159 (2022).

375 8. Khoury, G. El *et al.* Bespoke affinity ligands for the purification of therapeutic proteins. *Pharm.*
376 *Bioprocess.* **3**, 139–152 (2015).

377 9. Owczarek, B., Gerszberg, A. & Hnatuszko-Konka, K. A Brief Reminder of Systems of Production and
378 Chromatography-Based Recovery of Recombinant Protein Biopharmaceuticals. *BioMed Research*
379 *International* vol. 2019 at https://doi.org/10.1155/2019/4216060 (2019).

380 10. Samaras, J. J., Micheletti, M. & Ding, W. Transformation of Biopharmaceutical Manufacturing

381 Through Single-Use Technologies: Current State, Remaining Challenges, and Future Development.
382 *Annu. Rev. Chem. Biomol. Eng.* **13**, 73–97 (2022).

383 11. Kuntz, I. D., Chen, K., Sharp, K. A. & Kollman, P. A. The maximal affinity of ligands. *Proc. Natl. Acad.*
384 *Sci. U. S. A.* **96**, 9997–10002 (1999).

385 12. Mouratou, B., Béhar, G. & Pecorari, F. Artificial affinity proteins as ligands of immunoglobulins.
386 *Biomolecules* **5**, 60–75 (2015).

387 13. Hais, I. M. Biospecific sorption, Prague, 1910: Emil Starkenstein (1884-1942). *J. Chromatogr. B*
388 *Biomed. Sci. Appl.* **376**, 5–9 (1986).

389 14. Rodriguez, E. L. *et al.* Affinity chromatography: A review of trends and developments over the past
390 50 years. *Journal of Chromatography B: Analytical Technologies in the Biomedical and Life Sciences*
391 vol. 1157 at https://doi.org/10.1016/j.jchromb.2020.122332 (2020).

392 15. Uriza, P. J. *et al.* Development of an Antigen Delivery Platform Using Lactobacillus acidophilus
393 Decorated With Heterologous Proteins: A Sheep in Wolf's Clothing Story. *Front. Microbiol.* **11**,
394 (2020).

395 16. Jumper, J. *et al.* Highly accurate protein structure prediction with AlphaFold. *Nature* **596**, 583 (2021).

396 17. Garduno, R. A., Phipps, B. M. & Kay, W. W. Physical and functional S-layer reconstitution in
397 Aeromonas salmonicida. *J. Bacteriol.* **177**, 2684–2694 (1995).

398 18. Mader, C., Huber, C., Moll, D., Sleytr, U. B. & Sára, M. Interaction of the Crystalline Bacterial Cell
399 Surface Layer Protein SbsB and the Secondary Cell Wall Polymer of Geobacillus stearothermophilus
400 PV72 Assessed by Real-Time Surface Plasmon Resonance Biosensor Technology. *J. Bacteriol.* **186**,
401 1758–1768 (2004).

402 19. Li, J., Hu, X., Yan, J. & Yuan, Z. Species-specific cell wall binding affinity of the S-layer proteins of
403 mosquitocidal bacterium Bacillus sphaericus C3-41. *Appl. Environ. Microbiol.* **75**, 3891–3895 (2009).

404 20. Lortal, S. *et al. S-layer of Lactobacillus helveticus atcc 12046: isolation, chemical characterization and*
405 *re-formation after extraction with lithium chloride Slayer of Lactobacillus helveticus ATCC 12046:*
406 *isolation, chemical characterization and re-formation after extraction with lithium chloride*. *Society*
407 *for General Microbiology* vol. 138 https://hal.inrae.fr/hal-02713428 (1992).

408 21. Fina Martin, J. *et al.* Exploring lectin-like activity of the S-layer protein of Lactobacillus acidophilus
409 ATCC 4356. *Appl. Microbiol. Biotechnol.* **103**, 4839–4857 (2019).

410 22. Kim, I. J., Xu, Y. & Nam, K. H. Spectroscopic Analysis of Fe Ion-Induced Fluorescence Quenching of
411 the Green Fluorescent Protein ZsGreen. *J. Fluoresc.* **31**, 307–314 (2021).

412 23. Richmond, T. A., Takahashi, T. T., Shimkhada, R. & Bernsdorf, J. Engineered metal binding sites on
413 green fluorescence protein. *Biochem. Biophys. Res. Commun.* **268**, 462–465 (2000).

414 24. Buxbaum, E. *Enzymes Are Biocatalysts*. *Fundamentals of Protein Structure and Function* (2015).
415 doi:10.1007/978-3-319-19920-7_4.

416 25. Baldo, B. A. Chimeric Fusion Proteins Used for Therapy: Indications, Mechanisms, and Safety. *Drug*
417 *Saf.* **38**, 455–479 (2015).

418 26. Fei Wen, Sheryl B. Rubin-Pitel, and H. Z. Engineering of Therapeutic Proteins.Chp7. 153–177 (2009).

419 27. Hsieh, C.-L. *et al.* Structure-based design of prefusion-stabilized SARS-CoV-2 spikes. *Science (80-.).*
420 **369**, 1501–1505 (2020).

421 28. Jumper, J. *et al.* Highly accurate protein structure prediction with AlphaFold. *Nature* **596**, 583–589
422 (2021).

423 29. Nadi, A. *et al.* Immobilisation of bacteria onto magnetic nanoparticles for the decolorisation and
424 degradation of azo dyes. *IET Nanobiotechnology* **13**, 144–149 (2019).

425

426 Figures

427 **Figure 1: Characterization of (H_6)-GFP-SLAP$_{TAG}$ binding to Bio-matrix.** (A) The AlphaFold2 model of (H_6)-GFP-
428 SLAP$_{TAG}$ fusion protein. AlphaFold2 predicted structure was automatically colored by the pLDDT confidence
429 measure. High accuracy is colored in blue while low accuracy in red. Despite SLAP$_{TAG}$ has not been crystallized,
430 structure prediction showed a good performance. (B) Figure compares (H_6)-GFP-SLAP$_{TAG}$ purification yield of
431 SLAP$_{TAG}$-based affinity chromatography for different temperatures of the binding process. (C) Figure
432 compares (H_6)-GFP-SLAP$_{TAG}$ purification yield of SLAP$_{TAG}$-based affinity chromatography for different times of
433 binding incubation. (D) Adsorption isotherm of (H_6)-GFP-SLAP$_{TAG}$ onto Bio-Matrix. Asterisk (****) denotes
434 significant difference using the ANOVA method, Bonferroni test ($p < 0.0001$).

435 **Figure 2: Characterization of (H_6)-GFP-SLAP$_{TAG}$ elution.** (A) Figure compares (H_6)-GFP-SLAP$_{TAG}$ purification
436 yield of SLAP$_{TAG}$-based affinity chromatography for different temperatures of elution. (B) Figure compares
437 (H_6)-GFP-SLAP$_{TAG}$ purification yield of SLAP$_{TAG}$-based affinity chromatography for different times of elution
438 incubation. (C) Figure compares (H_6)-GFP-SLAP$_{TAG}$ purification yield of SLAP$_{TAG}$-based affinity chromatography
439 system for different eluents. Asterisk denotes significant difference using the ANOVA method, Bonferroni
440 test (*** $p = 0,0003$; **** $p < 0.0001$).

441 **Figure 3: Optimized protocol for (H_6)-GFP-SLAP$_{TAG}$ purification using the Bio-matrix and comparison with**
442 **the high-performance Ni^{2+}-charged agarose matrix**. (A) Graphical description of the SLAP$_{TAG}$-based affinity
443 chromatography protocol. (B) Confocal microscopy of the Bio-Matrix. *Bacillus subtilis* red native
444 autofluorescence is observed. (C) Confocal microscopy of (H_6)-GFP-SLAP$_{TAG}$ bound to the Bio-Matrix. GFP is
445 visualized on the *Bacillus* surface. (D) Confocal microscopy of the Bio-Matrix after elution of (H_6)-GFP-SLAP$_{TAG}$.
446 (E) Tubes containing purification fractions seen under UV light. GFP input fluorescence is recovered in the
447 eluate. (F) Coomassie blue staining analysis of (H_6)-GFP-SLAP$_{TAG}$ scaled purification. BM = Bio-Matrix; MK =
448 protein marker (KDa); IN = input; FT = flowthrough; W = wash; E = elution. (G) Immobilized metal affinity
449 chromatography (IMAC) and SLAP$_{TAG}$-based affinity chromatography system are compared in their capacity

450 to purify (H_6)-GFP-SLAP$_{TAG}$. Relative fluorescence of total (H_6)-GFP-SLAP$_{TAG}$ recovered in elution fraction is
451 shown.

452 **Figure 4: Representation of SLAP-tagged recombinant protein structure.** Lys = bacteriophage T4 lysozyme;
453 GFP = *Aequorea victoria* green fluorescent protein; GST = glutathione-s-transferase; HRV-3c = human
454 Rhinovirus 3C Protease; EspA = *E. coli* EspA protein; Omp19 = *B. abortus* Omp19 protein; MBP = maltose-
455 binding protein; Gal8 = mouse Galectin-8; EITH7 = EspA, Intimin and Tir fusion protein from the Shiga-toxin
456 producing *E. coli*; Spike = SARS-CoV2 Spike protein.

457 **Figure 5: Analysis of different SLAP-tagged protein purifications expressed in *E. coli*.** Coomassie Blue stained
458 SDS-PAGE of purification fractions of SLAP$_{TAG}$-based affinity chromatography for (A) FliC-SLAP$_{TAG}$ (B) EspA-
459 SLAP$_{TAG}$ (C) Gal8-SLAP$_{TAG}$ (D) GST-SLAP$_{TAG}$ (E) Lys -SLAP$_{TAG}$ (F) Omp19-SLAP$_{TAG}$ (G) EITH7-SLAP$_{TAG}$ (H) SLAP$_{ASE}$
460 (human rhinovirus 3c fused to SLAP$_{TAG}$). MK = protein marker (KDa); IN = input; FT = flowthrough; W = wash;
461 E = elution.

462 **Figure 6: Western blot analysis of purification of SLAP-tagged proteins using different expression systems.**
463 (A) Purification of SLAP$_{ASE}$ (human rhinovirus 3c fused to SLAP$_{TAG}$) protease expressed in *Pichia pastoris*. (B)
464 Purification of SARS CoV2 Spike-SLAP$_{TAG}$ protein expressed in HEK293 cells. MK = protein marker (KDa); IN =
465 input; FT = flowthrough; W = wash; E = elution.

466 **Figure 7: Analysis of Bio-Matrix stability in time and reuse.** (A) The figure compares (H_6)-GFP-SLAP$_{TAG}$
467 purification yield of SLAP$_{TAG}$-based affinity chromatography at different times when it is conserved at -20ºC.
468 (B) Figure compares (H_6)-GFP-SLAP$_{TAG}$ purification yield of SLAP$_{TAG}$-based affinity chromatography for
469 different cycles of reuse. Asterisk denotes significant difference using the ANOVA method, Bonferroni test
470 (** $p = 0{,}0059$; *** $p = 0{,}0002$; **** $p < 0.0001$)

471

472 **Figure 8: SLAP$_{TAG}$ removal.** (A) Graphical description of the protocol to remove the SLAP$_{TAG}$ using SLAP$_{TAG}$-
473 based affinity chromatography. SDS-PAGE of purification fractions of SLAP$_{TAG}$ removal protocol stained with

474 Coomassie blue solution (B) or under UV light (C). Western Blot of purification fractions of $SLAP_{TAG}$ removal
475 protocol revealed with anti- $SLAP_{TAG}$ (D) or anti-GFP (E) antibodies. $SLAP_{ASE}$ = purified protease; IN = input; FT
476 = flowthrough; E = elution; MK = protein marker (KDa)

477

478 **Figure 9: GFP-$SLAP_{TAG}$ purification using Magnetic Bio-Matrix.** (A) Graphical description of the purification
479 protocol for magnetic Bio-Matrix. (B) Photo of 1,5 tubes ml containing fractions of GFP-$SLAP_{TAG}$ magnetic
480 purification under UV light. (BM_{mag} = magnetic Bio-Matrix; IN = input; FT = flowthrough; W = wash; E =
481 elution)

482

483

484

485 TABLE 1

Strain		
E. coli DH5α	F−ϕ80*lac*ZΔM15 Δ(*lac*ZYA-*arg*F) U169 *rec*A1 *end*A1 *hsd*R17(rK−, mK+) *pho*A *sup*E44λ- *thi*-1 *gyr*A96 *rel*A1	Invitrogen
E. coli BL21 Codon plus	[*omp*T *hsd*S(rB– mB–) *dcm* + Tcr *gal* λ (DE3) *end*A Hte Cmr]	Stratagen
B. subtilis	Wild type strain var. *natto*	ATCC 15245
Pichia pastoris	*P. pastoris* strain GS115	BioRad, USA
Plasmid		
pET28-eGFP-SlpA	A vector containing GFP gene from *Aequorea victoria* fused to $SLAP_{TAG}$	[21]
pET22-eGFP-SlpA	A vector containing GFP gene from *Aequorea victoria* fused to LEVLFQGP sequence and $SLAP_{TAG}$	This study
pGEX-SlpA	A vector containing GST form *Shitosoma japonicum* fused to $SLAP_{TAG}$	[15]
pLC3-EITH7-SlpA	A vector containing EspA-Intimin-Tir fusioned genes from STEC *E. coli* fused to $SLAP_{TAG}$	[15]
pLC3-Omp19-SlpA	A vector containing Omp19 gene from *Brucella abortus* fused to $SLAP_{TAG}$	[15]
pLC3-FliC-SlpA	A vector containing FliC gene from *Salmonella enterica* fused to $SLAP_{TAG}$	[15]
pLC3-Gal8-SlpA	A vector containing Gal8 gene from *Mus musculus* fused to $SLAP_{TAG}$	[15]
pET28-Lys-SlpA	A vector containing Lysozyme gene from *Gallus gallus* fused to $SLAP_{TAG}$	This study
pMAL-c5X-HRV3c-SlpA	A vector containing human rhinovirus (HRV) type 14 3C protease gene fused to $SLAP_{TAG}$ (SLAPase)	This study
pGEX-2T-EspA-SlpA	A vector containing the EspA gene from STEC *E. coli* fused to $SLAP_{TAG}$	This study
pPICZalphaB-HRV3c-SlpA	A vector containing human rhinovirus (HRV) type 14 3C protease gene fused to $SLAP_{TAG}$ (SLAPase)	This study
Addgene #154754	A vector containing the sequence of SARS CoV2 Spike ectodomain Hexa-pro	[27]
pSpike-$SLAP_{TAG}$	Plasmid Addgene #154754 fused with the $SLAP_{TAG}$	This study
pLysS	Vector for expression of T7 lysozyme.	Novagene

486

Figure 1

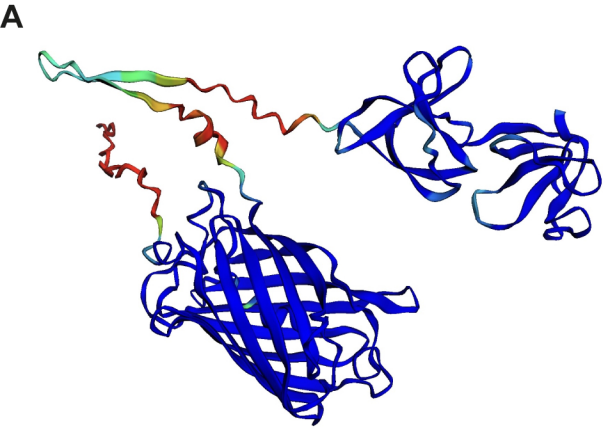
A

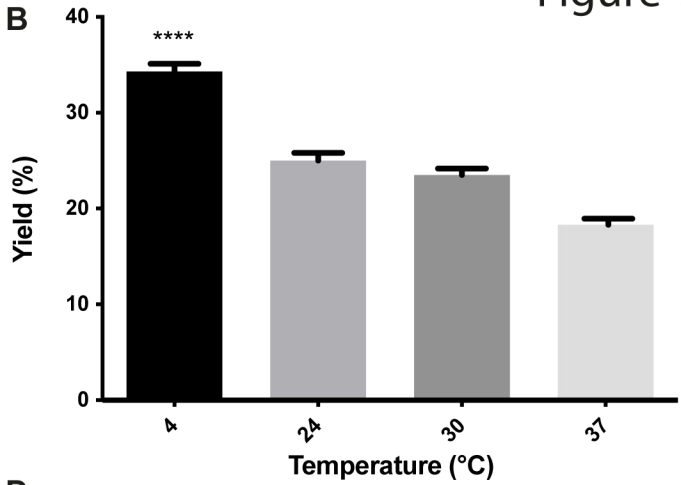
B
****
Yield (%)
0
10
20
30
40
4
24
30
37
Temperature (°C)

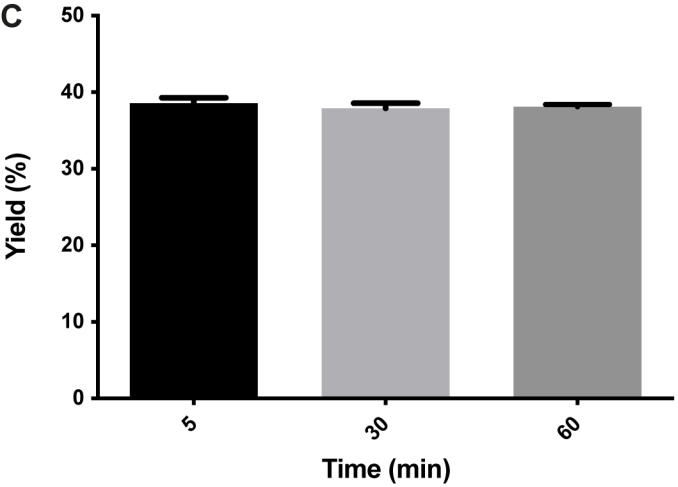
C
Yield (%)
0
10
20
30
40
50
5
30
60
Time (min)

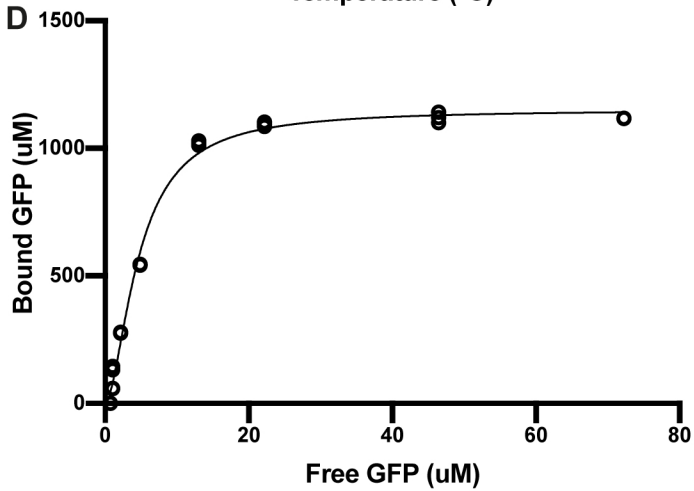
D
Bound GFP (uM)
0
500
1000
1500
0
20
40
60
80
Free GFP (uM)

Figure 2

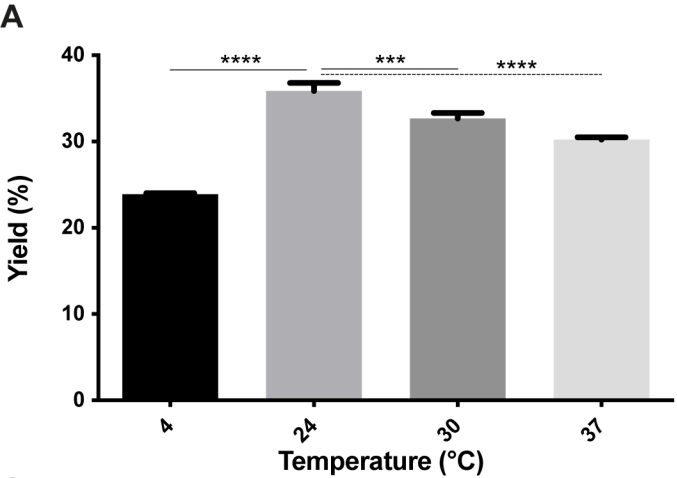
A
****
***
****
Yield (%)
40
30
20
10
0
4
24
30
37
Temperature (°C)

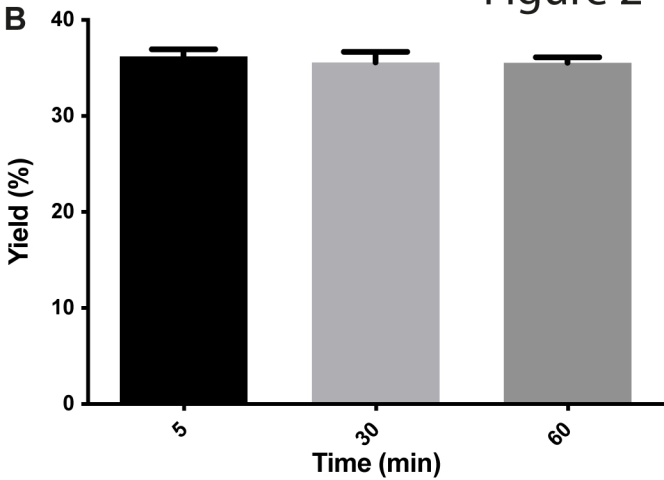
B
Yield (%)
40
30
20
10
0
5
30
60
Time (min)

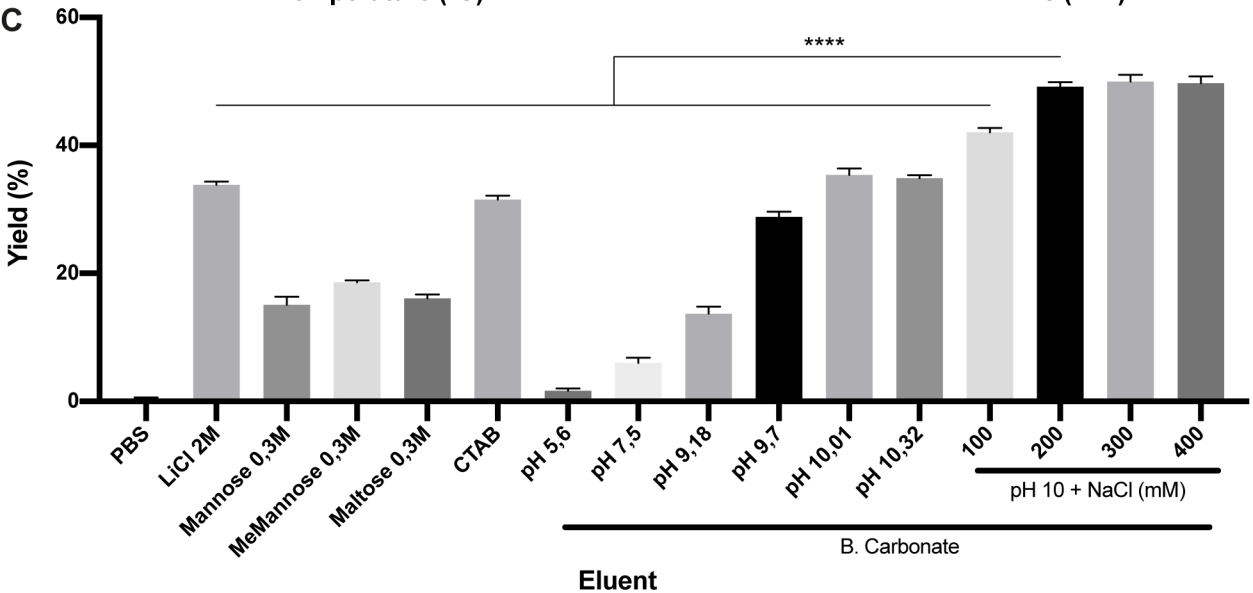
C
****
Yield (%)
60
40
20
0
PBS
LiCl 2M
Mannose 0,3M
MeMannose 0,3M
Maltose 0,3M
CTAB
pH 5,6
pH 7,5
pH 9,18
pH 9,7
pH 10,01
pH 10,32
100
200
300
400
pH 10 + NaCl (mM)
B. Carbonate
Eluent

Figure 3

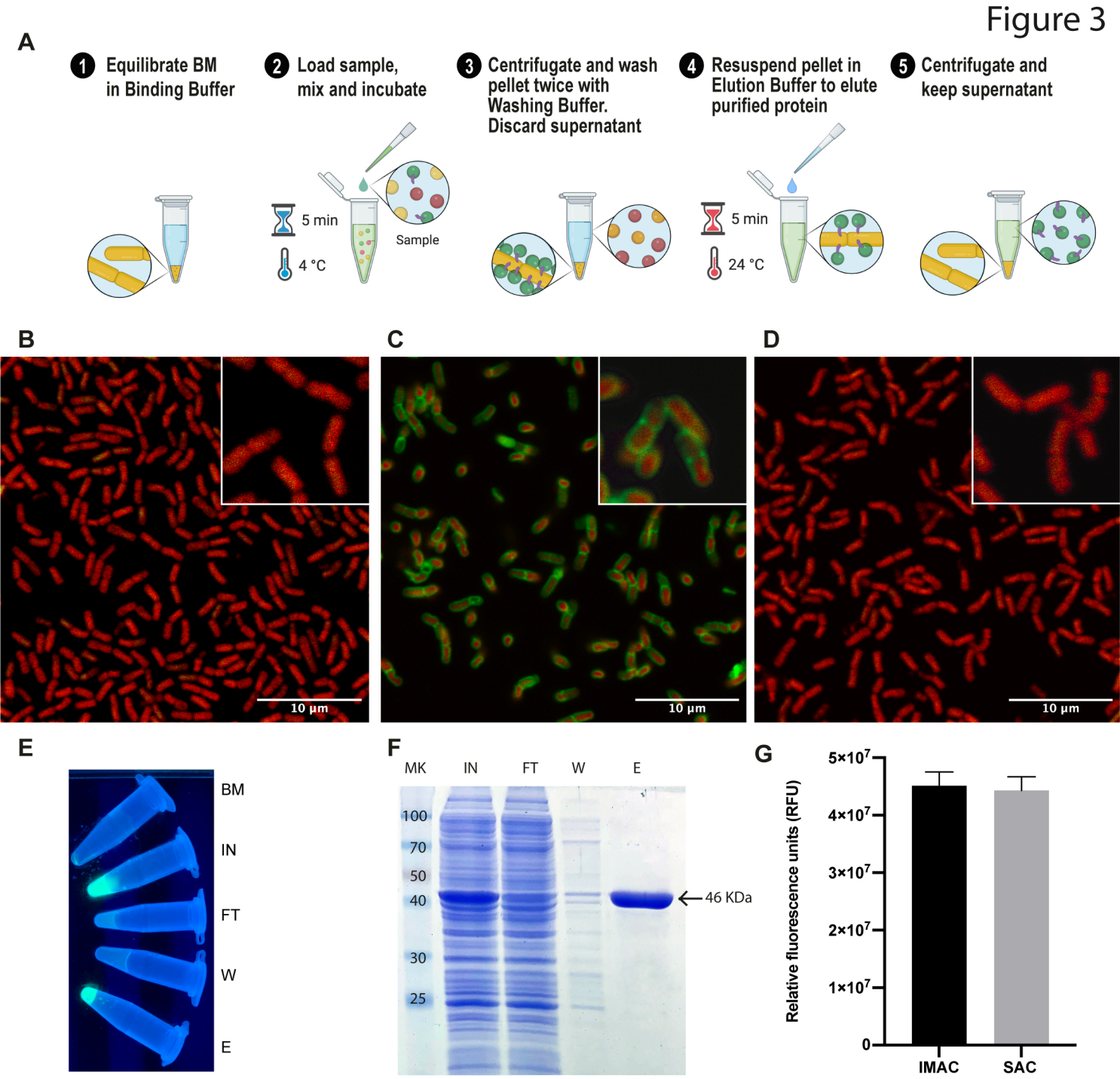
A
1 Equilibrate BM in Binding Buffer
2 Load sample, mix and incubate
5 min
4 °C
Sample
3 Centrifugate and wash pellet twice with Washing Buffer. Discard supernatant
4 Resuspend pellet in Elution Buffer to elute purified protein
5 min
24 °C
5 Centrifugate and keep supernatant
B
C
D
10 µm
10 µm
10 µm
E
BM
IN
FT
W
E
F
MK
IN
FT
W
E
100
70
50
40
30
25
46 KDa
G
Relative fluorescence units (RFU)
5×10^7
4×10^7
3×10^7
2×10^7
1×10^7
0
IMAC
SAC

Figure 4

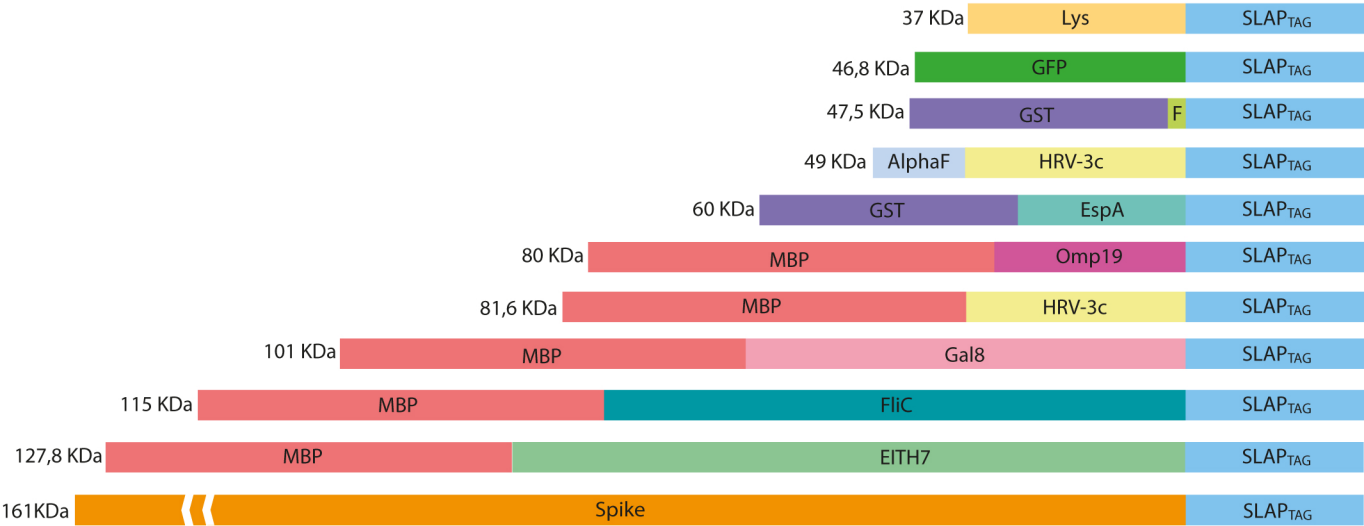
37 KDa
Lys
SLAP$_{TAG}$
46,8 KDa
GFP
SLAP$_{TAG}$
47,5 KDa
GST
F
SLAP$_{TAG}$
49 KDa
AlphaF
HRV-3c
SLAP$_{TAG}$
60 KDa
GST
EspA
SLAP$_{TAG}$
80 KDa
MBP
Omp19
SLAP$_{TAG}$
81,6 KDa
MBP
HRV-3c
SLAP$_{TAG}$
101 KDa
MBP
Gal8
SLAP$_{TAG}$
115 KDa
MBP
FliC
SLAP$_{TAG}$
127,8 KDa
MBP
EITH7
SLAP$_{TAG}$
161KDa
Spike
SLAP$_{TAG}$

Figure 5

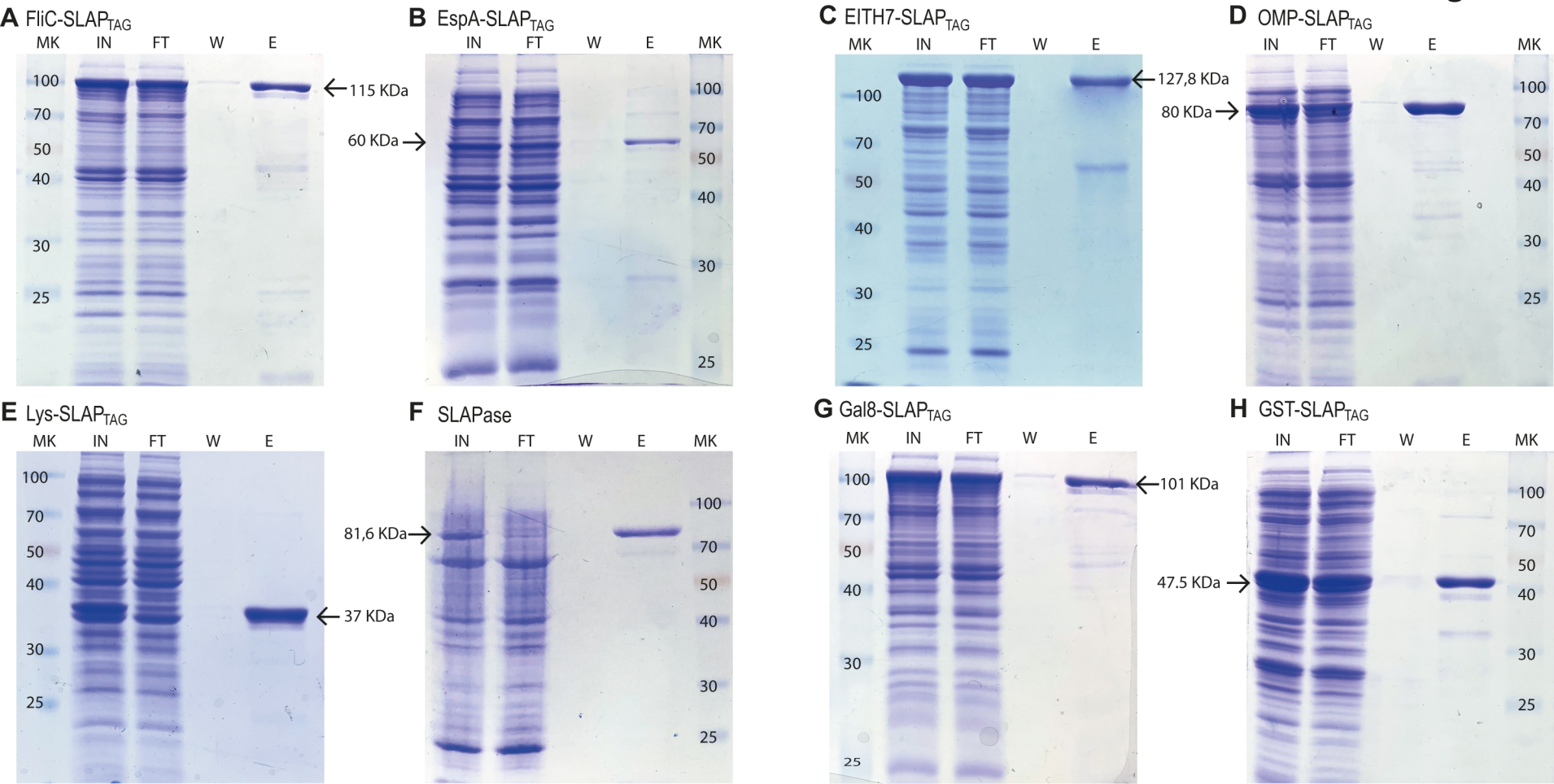
A FliC-SLAP$_{TAG}$
MK IN FT W E
100 70 50 40 30 25
115 KDa
B EspA-SLAP$_{TAG}$
IN FT W E MK
60 KDa
100 70 50 40 30 25
C EITH7-SLAP$_{TAG}$
MK IN FT W E
127,8 KDa
100 70 50 40 30 25
D OMP-SLAP$_{TAG}$
IN FT W E MK
80 KDa
100 70 50 40 30 25
E Lys-SLAP$_{TAG}$
MK IN FT W E
100 70 50 40 30 25
37 KDa
F SLAPase
IN FT W E MK
81,6 KDa
100 70 50 40 30 25
G Gal8-SLAP$_{TAG}$
MK IN FT W E
101 KDa
100 70 50 40 30 25
H GST-SLAP$_{TAG}$
IN FT W E MK
47.5 KDa
100 70 50 40 30 25

Figure 6

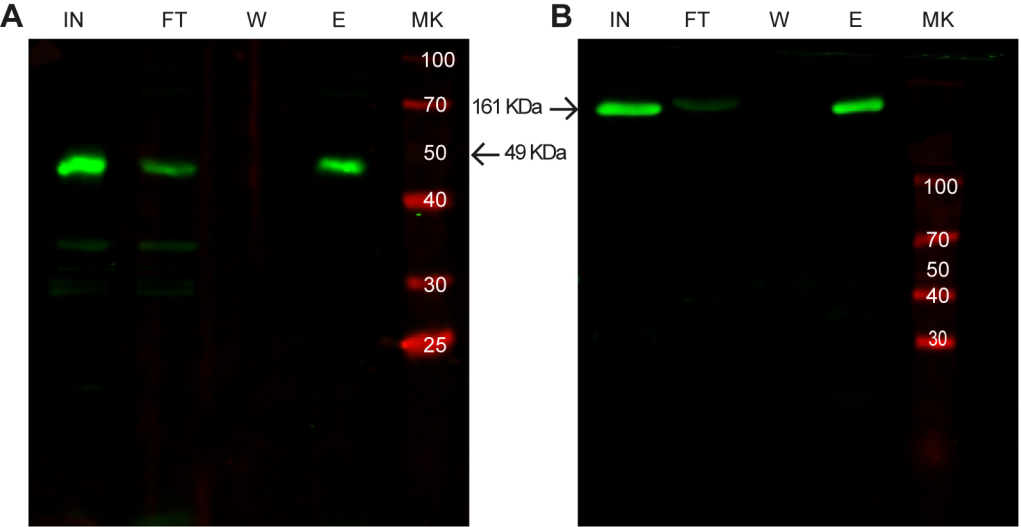
A
IN
FT
W
E
MK
100
70
50
40
30
25
161 KDa
49 KDa
B
IN
FT
W
E
MK
100
70
50
40
30

Figure 7

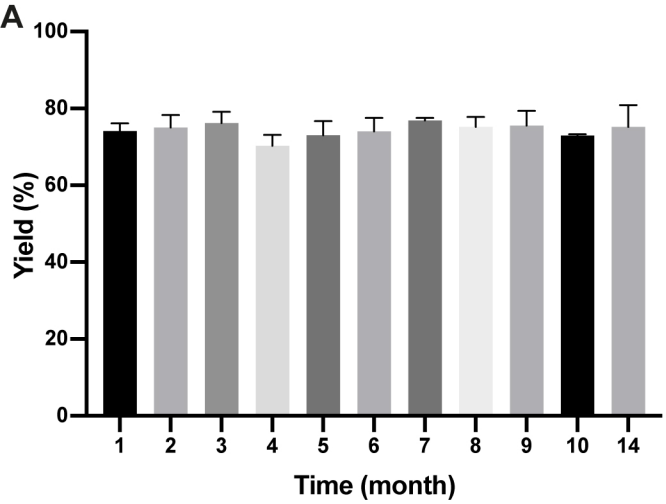
A
100
80
60
40
20
0
Yield (%)
1
2
3
4
5
6
7
8
9
10
14
Time (month)

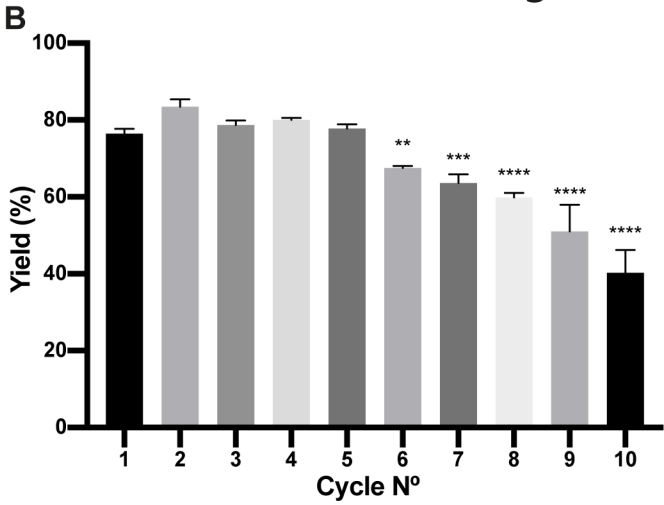
B
100
80
60
40
20
0
Yield (%)
**
***
****
****
****
1
2
3
4
5
6
7
8
9
10
Cycle Nº

Figure 8

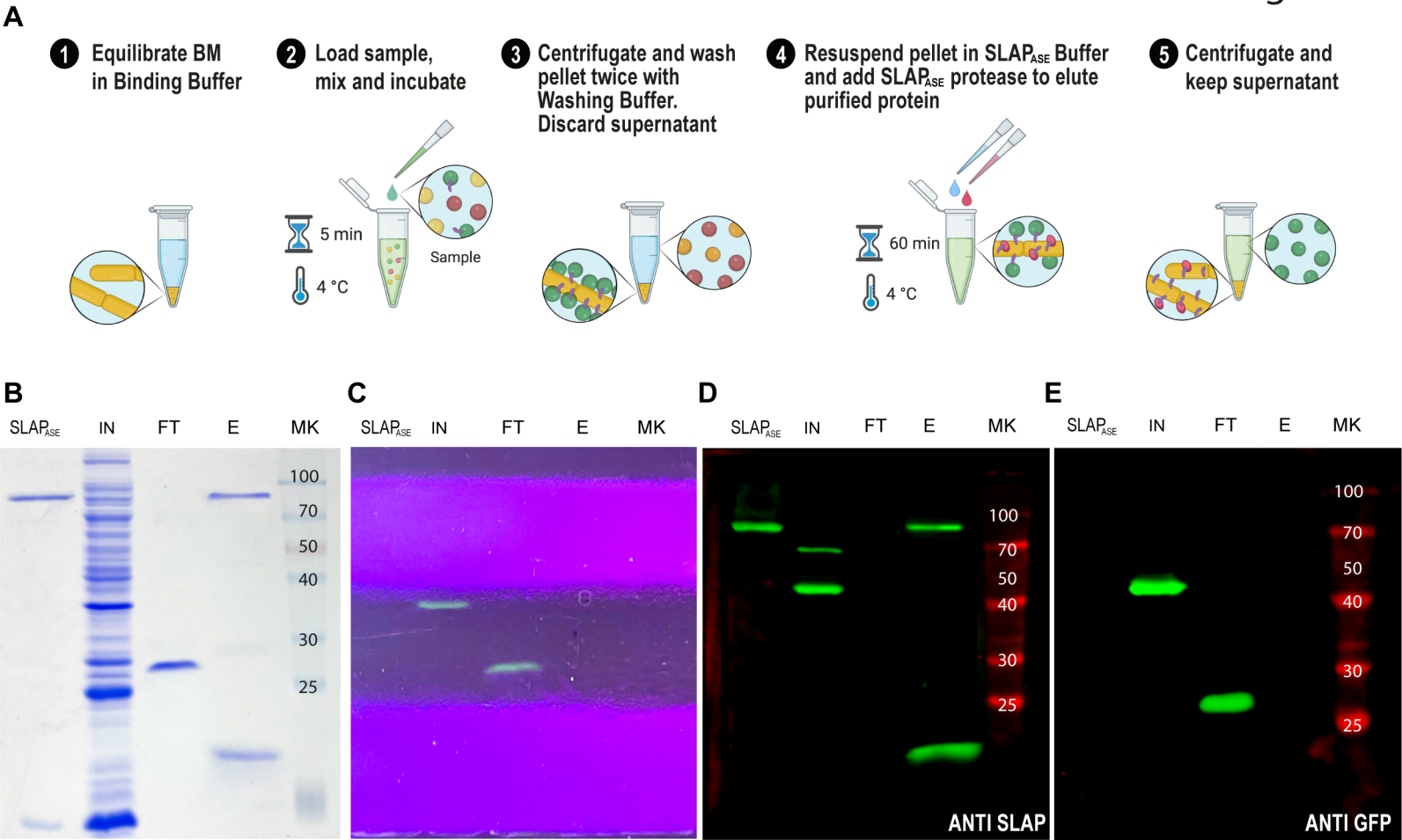
A
1 Equilibrate BM in Binding Buffer
2 Load sample, mix and incubate
5 min
4 °C
Sample
3 Centrifugate and wash pellet twice with Washing Buffer. Discard supernatant
4 Resuspend pellet in SLAPASE Buffer and add SLAPASE protease to elute purified protein
60 min
4 °C
5 Centrifugate and keep supernatant
B
SLAPASE IN FT E MK
100
70
50
40
30
25
C
SLAPASE IN FT E MK
D
SLAPASE IN FT E MK
100
70
50
40
30
25
ANTI SLAP
E
SLAPASE IN FT E MK
100
70
50
40
30
25
ANTI GFP

Figure 9

A

1 Equilibrate BM_{mag} in Binding Buffer

2 Load samble, mix and incubate

3 Transfer to magnete and wash pellet twice. Discard supernatant

4 Resuspend pellet in Elution Buffer to elute purified protein

5 Transfer to magnete and keep supernatant

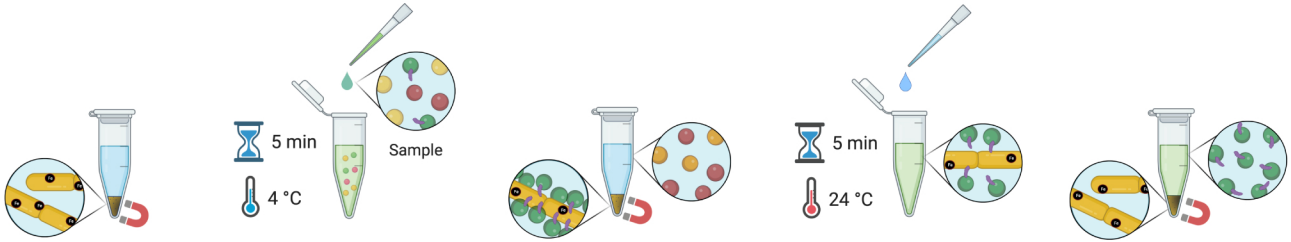

B

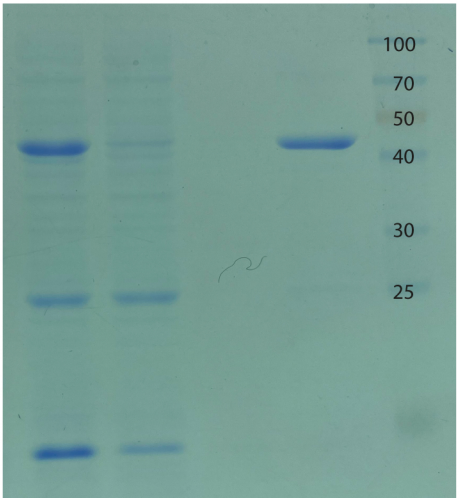
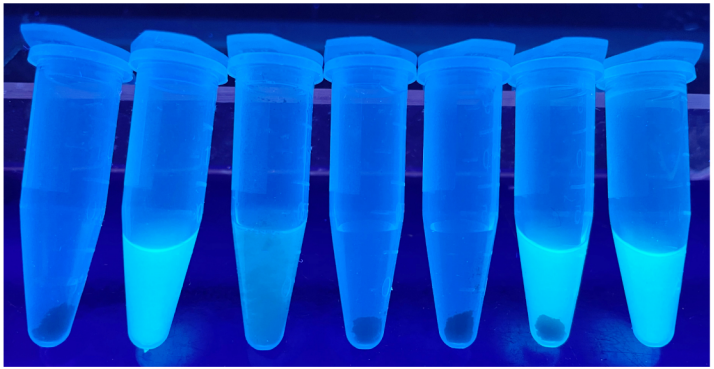
C